*Eur. J. Biochem.* **269**, 4418–4426 (2002) © FEBS 2002 doi:10.1046/j.1432-1033.2002.03125.x

# Elucidation of the role of fructose 2,6-bisphosphate in the regulation of glucose fluxes in mice using *in vivo* $^{13}$C NMR measurements of hepatic carbohydrate metabolism

**In-Young Choi[1], Chaodong Wu[2], David A. Okar[2], Alex J. Lange[2] and Rolf Gruetter[1,3]**

*Departments of Radiology[1], Biochemistry, Molecular Biology and Biophysics[2], Neuroscience[3], University of Minnesota Medical School, Minneapolis, MN, USA*

Fructose 2,6-bisphosphate (Fru-2,6-$P_2$) plays an important role in the regulation of major carbohydrate fluxes as both allosteric activator and inhibitor of target enzymes. To examine the role of Fru-2,6-$P_2$ in the regulation of hepatic carbohydrate metabolism *in vivo*, Fru-2,6-$P_2$ levels were elevated in ADM mice with adenovirus-mediated overexpression of a double mutant bifunctional enzyme, 6-phosphofructo-2-kinase/fructose-2,6-bisphosphatase ($n = 6$), in comparison to normal control mice (control, $n = 6$). The rates of hepatic glycogen synthesis in the ADM and control mouse liver *in vivo* were measured using new advances in $^{13}$C NMR including 3D localization in conjunction with [1-$^{13}$C]glucose infusion. In addition to glycogen C1, the C6 and C2–C5 signals were measured simultaneously for the first time *in vivo*, which provide the basis for the estimation of direct and indirect synthesis of glycogen in the liver. The rate of label incorporation into glycogen C1 was not different between the control and ADM group, whereas the rate of label incorporation into glycogen C6 signals was in the ADM group 5.6 ± 0.5 μmol·g$^{-1}$·h$^{-1}$, which was higher than that of the control group of 3.7 ± 0.5 μmol·g$^{-1}$·h$^{-1}$ ($P < 0.02$). The rates of net glycogen synthesis, determined by the glycogen C2–C5 signal changes, were twofold higher in the ADM group ($P = 0.04$). The results provide direct *in vivo* evidence that the effects of elevated Fru-2,6-$P_2$ levels in the liver include increased glycogen storage through indirect synthesis of glycogen. These observations provide a key to understanding the mechanisms by which elevated hepatic Fru-2,6-$P_2$ levels promote reduced hepatic glucose production and lower blood glucose in diabetes mellitus.

*Keywords*: NMR; *in vivo*; fructose-2, 6-bisphosphate; glycogen; mouse liver.

The regulation of carbohydrate metabolism in the liver is important for blood glucose homeostasis by controlling hepatic glucose production. This involves an intricate regulation of metabolic pathways, such as glycolysis, gluconeogenesis, glycogenesis and glycogenolysis in the liver [1,2]. The balance of these pathways is severely altered in patients with type II diabetes mellitus contributing to chronically elevated plasma glucose concentrations. Therefore, an understanding of the regulation of these fluxes can provide important insights into the mechanisms and potential treatment of diabetes.

The rates of glycolysis and gluconeogenesis are important in the rate of hepatic glucose production. Fructose-2,6-bisphosphate (Fru-2,6-$P_2$) plays an important role through its reciprocal allosteric effects on two critical enzymes, 6-phosphofructo-1-kinase and fructose-1,6-bisphosphatase (reviewed in [3]). Fru-2,6-$P_2$ activates phosphofructo-1-kinase to stimulate glycolysis and inhibits fructose-1,6-bisphosphatase to reduce gluconeogenesis. Synthesis as well as degradation of Fru-2,6-$P_2$ are controlled by the bifunctional enzyme 6-phosphofructo-2-kinase/fructose-2,6-bisphosphatase [4,5], providing a switch between glycolytic and gluconeogenic pathways in the liver [3,6,7]. For example, when the insulin/glucagon ratio is high, the enzyme is dephosphorylated at Ser32, its 6-phosphofructo-2-kinase activity is enhanced and the bisphosphatase activity is inhibited, resulting in a net synthesis of Fru-2,6-$P_2$ from fructose 6-phosphate and ATP [5]. On the other hand, when the insulin/glucagon ratio is low, 6-phosphofructo-2-kinase/fructose-2,6-bisphosphatase is phosphorylated by protein kinase A, which enhances the bisphosphatase activity and inhibits the kinase activity of the bifunctional enzyme, and Fru-2,6-$P_2$ is converted back to fructose 6-phosphate, thereby producing inorganic phosphate ($P_i$) [3].

Recently, we have shown that increasing Fru-2,6-$P_2$ content via adenovirus mediated 6-phosphofructo-2-kinase/fructose-2,6-bisphosphatase overexpression reduces hepatic glucose production and lowers blood glucose in both normal and diabetic mice [8,9]. The double mutant bifunctional enzyme used in that study has a mutation of Ser32→Ala, which prevents cAMP-dependent phosphorylation [10], and a mutation of His258→Ala, which diminishes bisphosphatase activity [11]. While the study confirmed that increased hepatic Fru-2,6-$P_2$ content can reduce blood glucose, it was not clear that the allosteric effects of this compound on 6-phosphofructo-1-kinase and fructose-1,6-bisphosphatase could fully account for the metabolic effects, especially with regard to the glycogen

*Correspondence to* R. Gruetter, Center for Magnetic Resonance Research, 2021 6th Street SE, Minneapolis, MN 55455, USA.
Fax: + 1 612 626 2004, Tel.: + 1 612 625-6582,
E-mail: gruetter@cmrr.umn.edu

*Abbreviations*: Fru-2,6-$P_2$, fructose 2,6-bisphosphate; TR, repetition time; TE, echo time.

(Received 14 March 2002, revised 10 July 2002, accepted 18 July 2002)

stores. In fact, it was observed that the increased hepatic Fru-2,6-$P_2$ was also correlated with an up-regulation of glucokinase and a down-regulation of glucose-6-phosphatase gene expression, suggesting that this biofactor may also be involved in balancing the uptake and release of glucose from the liver [8,9].

$^{13}$C NMR spectroscopy has been used to measure glucose and glycogen metabolism in respiring isolated liver cells [12,13] and perfused liver [12,14–17]. Recently, relative flux rates have been measured in humans [18–21]. However, quantification of absolute fluxes *in vivo* can be complicated by the fact that no well-defined three-dimensional localization method has been used for hepatic studies and by the limited amount of information available when measuring the glycogen C1 signal change alone, resulting only in net glycogen concentration measurements [22]. The present study presents several advances in the MR technology for the purpose of measuring hepatic glycogen metabolism. First, this is the first study to implement and use full three-dimensional localization of $^{13}$C NMR signals of glycogen in the intact liver *in vivo*. Second, during infusion of [1-$^{13}$C]glucose, label incorporation was observed not only into the C1 of glycogen but also the C6, which can only occur by label scrambling at the level of the trioses. In addition, the signals of glycogen C2–C5 were detected, possibly reflecting changes in natural abundance glycogen (i.e. net glycogen concentration changes). In the present study, we used these advances in $^{13}$C NMR: (a) to measure the rates of hepatic glycogen synthesis in normal animals treated with adenovirus encoding the double mutant rat liver bifunctional enzyme in comparison with normal (nondiabetic) control animals; and (b) to assess the role of hepatic Fru-2,6-$P_2$ in controlling glucose and/or glycogen metabolism.

## MATERIALS AND METHODS

### Animal preparation

The study was conducted according to the guidelines of the Institutional Animal Care and Use Committee (IACUC) of the University of Minnesota. Twelve male 129J mice (Jackson Laboratory, Bar Harbor, ME, USA) were studied after an overnight fast with access to water ($n = 12$, 24.7 ± 0.5 g, mean ± SE). Six normal control animals were studied without any treatment (control group, 23.3 ± 0.2 g body weight). Six mice were treated with an adenovirus vector containing the cDNA encoding mutant rat liver bisphosphatase-deficient 6-phosphofructo-2-kinase/fructose-2,6-bisphosphatase 7 days prior to the study [8] to overexpress the double mutant rat liver bifunctional enzyme (ADM group, 26.0 ± 0.5 g body weight).

All animals were initially anesthetized using a bolus injection of pentobarbital (Abbott Laboratory, North Chicago, IL, USA) solution (10 mg·mL$^{-1}$) intraperitoneally (60 mg·kg$^{-1}$). Two catheters were inserted into the tail veins, one for the administration of pentobarbital and one for the infusion of glucose. A third catheter was placed intraperitoneally as an alternative means of glucose administration should the tail vein fail, which was the case in only three animals, the data of which were included. After the lines were inserted, pentobarbital was infused continuously at 4.8–6.0 mg·kg$^{-1}$·h$^{-1}$. The animals were secured in a home-built holder and placed in an acrylic holder attached to an insert in the gradient coil. Body temperature was maintained at 37.0 ± 0.5 °C with a warm water circulation system based on a feedback obtained from a temperature probe placed on the abdomen of the mice (Cole Parmer, Vernon Hills, IL, USA). 99% enriched [1-$^{13}$C]D-glucose (20% w/v solution, Isotec Inc., Miamisburg, OH) was infused either intravenously through the tail vein ($n = 9$) or intraperitoneally ($n = 3$) with an initial bolus of approximately 50 mg·kg$^{-1}$·min$^{-1}$ such that blood glucose was rapidly raised to 10–12 mM. Intraperitoneal and intravenous infusion protocols were optimized in benchtop experiments to provide a similar rise in plasma glucose in the same short time. The glucose infusion rate was adjusted continuously thereafter to maintain a stable liver glucose signal.

### NMR methods

All experiments were performed on a 9.4 Tesla, 31 cm bore horizontal magnet (Magnex Scientific), interfaced to a Varian INOVA console (Palo Alto, CA, USA). An actively shielded gradient coil (Magnex Scientific, Abingdon, UK) with an 11 cm inner diameter was used. A custom-built quadrature $^1$H surface RF coil (14 mm diameter) and a linear three-turn $^{13}$C coil (12 mm diameter) was used as a transceiver for $^1$H NMR and $^{13}$C NMR spectroscopy built according to a previously described design [23]. A sphere filled with 99% $^{13}$C enriched formic acid was placed at the center of the $^{13}$C coil as an external reference and the coil was placed on the animal's abdomen directly over the liver. The position of the liver was identified in gradient-recalled echo magnetic resonance images (repetition time, TR = 10 ms, echo time, TE = 5 ms). The volume of interest was placed in the mouse liver with typical volume sizes of 300–430 μL. Three-dimensional localization based on a recently described method [24] that uses outer volume saturation ensured complete elimination of signals from outside of the volume of interest. The localized signals of glycogen and glucose were acquired with spectrometer offset set to 100 p.p.m. (64 scans with repetition time, TR = 1 s). All data were processed with 15 Hz or 20 Hz exponential multiplication, zero filling, fast Fourier transformation and zero-order phase correction.

Glycogen and glucose resonances were quantified using the external reference method as described previously [25,26]. In short, $^{13}$C NMR signals of glycogen and glucose *in vivo* were quantified by comparison with the measurements of phantoms containing solutions of ≈400 mM natural abundance oyster glycogen and 0.9 mM of 99% enriched [1-$^{13}$C]D-glucose. The phantom measurements were performed under identical experimental conditions as the *in vivo* experiments. Coil loading effects on sensitivity and radio frequency (RF) power were assessed by measuring the 180° pulse duration on the $^{13}$C formic acid signal. Differences in saturation factors including $T_1$ relaxation and the nuclear Overhauser effect (NOE) were assessed *in vivo* and in phantom experiments.

### Assessment of the overexpression of the double mutant bifunctional enzyme.

The adenovirus infusion resulted in overexpression of the bifunctional enzyme, which was assessed as described previously [8]. The bifunctional enzyme was significantly

increased after tail-vein infusion of adenovirus within 3 days and peaked between 5 and 7 days post infusion. The treatment was accompanied by elevated hepatic Fru-2,6-$P_2$ levels and lowered blood glucose. In addition, liver glycogen content was reduced in response to the overexpression of ADM relative to the untreated normal control animals [8]. Because a direct assessment of the ADM or Fru-2,6-$P_2$ content in the liver requires tissue extraction, indirect evidence of ADM overexpression in the liver was assessed prior to the infusion of glucose from the fasting blood glucose using a glucose oxidase method (Precision glucometer; Medisense Inc. Waltham, MA, USA) and hepatic glycogen content determined by natural abundance *in vivo* $^{13}$C NMR spectroscopy (see above). This approach is direct evidence for overexpression of the bifunctional enzyme, because the protocol was entirely identical to that used in our previous study [8,9].

### Measurement of the rate of $^{13}$C label incorporation into glycogen in the liver

Label incorporation into the glycogen C1 reflects glycogen synthesis via the direct pathway (glucose→glucose-6-phosphate→glycogen), whereas label incorporation into the glycogen C6 reflects activity in the indirect pathway due to label scrambling at the triose level (glucose→glucose-6-phosphate→pyruvate (triose level)→glycogen), which is predominantly a hepatic process. Changes in $^{13}$C-labeled glycogen C1 and C6 concentration (rate of $^{13}$C label incorporation, $\Delta^{13}\mathrm{Glyc}_1$ and $\Delta^{13}\mathrm{Glyc}_6$) were calculated by linear regression at specific time points. Data points were calculated from $^{13}$C NMR spectra with a temporal resolution of 4–8 min as a result of averaging spectra collected with $\approx$1 min temporal resolution. $^{13}$C glycogen changes were calculated at $\approx$2, $\approx$3, and $>$4 h from the start of glucose infusion. For the calculation of glycogen C6 changes, data acquired within 1 h of the start of the glucose infusion was not included to avoid any influence of transient changes in the isotopic enrichment.

The rates of $^{13}$C incorporation into glycogen were expressed as a function of precursor metabolite, glucose-6-phosphate (Glc6*P*), according to standard tracer methodology [27]:

$$\frac{\mathrm{d}[^{13}\mathrm{Glyc}_1]}{\mathrm{d}t}(t) = V_{\mathrm{syn}} \cdot \frac{[^{13}\mathrm{Glc6}P_1]}{[\mathrm{Glc6}P]}(t) - V_{\mathrm{phos}} \cdot \frac{[^{13}\mathrm{Glyc}_1]}{[\mathrm{Glyc}]}(t) \quad (1)$$

$$\frac{\mathrm{d}[^{13}\mathrm{Glyc}_6]}{\mathrm{d}t}(t) = V_{\mathrm{syn}} \cdot \frac{[^{13}\mathrm{Glc6}P_6]}{[\mathrm{Glc6}P]}(t) - V_{\mathrm{phos}} \cdot \frac{[^{13}\mathrm{Glyc}_6]}{[\mathrm{Glyc}]}(t) \quad (2)$$

$$V_{\mathrm{net}} = V_{\mathrm{syn}} - V_{\mathrm{phos}} \quad (3)$$

$V_{\mathrm{syn}}$, $V_{\mathrm{phos}}$ and $V_{\mathrm{net}}$ represent the flux through glycogen synthase, phosphorylase, and the rate of net glycogen synthesis, respectively. $^{13}\mathrm{Glyc}_1$ and $^{13}\mathrm{Glyc}_6$ represent $^{13}$C-labeled glycogen C1 and C6 concentration, and $^{13}\mathrm{Glc6}P_1$ and $^{13}\mathrm{Glc6}P_6$ represent $^{13}$C-labeled glucose-6-phosphate C1 and C6 concentration, respectively. Because the rate of label incorporation into glycogen C1, the relative isotopic enrichments of glycogen C1 and C6, and the net glycogen synthesis rate were measured, Eqns (1), (2) and (3) can be rearranged to determine $V_{\mathrm{syn}}$ and the isotopic enrichment of Glc6*P* in terms of $V_{\mathrm{phos}}$ as:

$$\frac{[^{13}\mathrm{Glc6}P_1]}{[\mathrm{Glc6}P]}(t) = \frac{\frac{\mathrm{d}[^{13}\mathrm{Glyc}_1]}{\mathrm{d}t}(t) + V_{\mathrm{phos}} \cdot \frac{[^{13}\mathrm{Glyc}_1]}{[\mathrm{Glyc}]}(t)}{V_{\mathrm{net}} + V_{\mathrm{phos}}} \quad (4)$$

$$\frac{[^{13}\mathrm{Glc6}P_6]}{[\mathrm{Glc6}P]}(t) = \frac{\frac{\mathrm{d}[^{13}\mathrm{Glyc}_6]}{\mathrm{d}t}(t) + V_{\mathrm{phos}} \cdot \frac{[^{13}\mathrm{Glyc}_6]}{[\mathrm{Glyc}]}(t)}{V_{\mathrm{net}} + V_{\mathrm{phos}}} \quad (5)$$

For example, $V_{\mathrm{phos}}$ can be determined by measuring $^{13}$C-label dilution during unlabeled glucose infusion following the $^{13}$C-labeled glucose infusion, as we have shown recently for brain glycogen [26]. Eqns (4) and (5) can be rearranged to express a relative isotopic enrichment of G6P at the C1 and C6 positions:

$$\frac{[^{13}\mathrm{Glc6}P_6]}{[^{13}\mathrm{Glc6}P_1]} = \frac{\frac{\mathrm{d}[^{13}\mathrm{Glyc}_6]}{\mathrm{d}t}(t) + V_{\mathrm{phos}} \cdot \frac{[^{13}\mathrm{Glyc}_6]}{[\mathrm{Glyc}]}(t)}{\frac{\mathrm{d}[^{13}\mathrm{Glyc}_1]}{\mathrm{d}t}(t) + V_{\mathrm{phos}} \cdot \frac{[^{13}\mathrm{Glyc}_1]}{[\mathrm{Glyc}]}(t)} \quad (6)$$

Initially, the enrichment of glycogen is low ($[^{13}\mathrm{G1yc}_6]$/[Glyc] $<<$ 1) and the temporal changes are approximated by the slope of the linear regression, which can be used to approximate Eqn (6) as follows:

$$\frac{[^{13}\mathrm{Glc6}P_6]}{[^{13}\mathrm{Glc6}P_1]} = \frac{\frac{\mathrm{d}[^{13}\mathrm{Glyc}_6]}{\mathrm{d}t}}{\frac{\mathrm{d}[^{13}\mathrm{Glyc}_1]}{\mathrm{d}t}} \cong \frac{[\Delta^{13}\mathrm{Glyc}_6]}{[\Delta^{13}\mathrm{Glyc}_1]} \approx \frac{[^{13}\mathrm{Glyc}_6]}{[^{13}\mathrm{Glyc}_1]} \quad (7)$$

Eqn (7) implies that the initial rate of label incorporation into glycogen C6 relative to the rate of label incorporation into glycogen C1 reflects the relative isotopic enrichment of Glc6*P* in the C6 relative to the C1 position. When the changes in glycogen C1 and C6 are linear with time, the differentials in the middle part of Eqn (7) can be replaced by the differences in label incorporation relative to that at time zero (which is close to zero) resulting in the right-hand approximation.

## RESULTS

Localized $^{13}$C NMR spectra were acquired from the volume of interest using a three-dimensional localization method. The location of the volume of interest, with a nominal volume of 400 μL was based on sagittal and transverse MR images of the mouse liver (Fig. 1A). Both the reduced blood glucose (fasting plasma glucose of 5.5 ± 0.3 mM in control vs. 4.1 ± 0.2 mM in ADM mice, mean ± SE) and initial liver glycogen content in the ADM mice were consistent with bifunctional enzyme overexpression in all experiments. During infusion of [1-$^{13}$C]D-glucose, signals from the glucose C1 resonances were immediately detected, along with natural abundance signals from glycerol C1 and C3 at 62.5 p.p.m. (Fig. 1B, bottom trace). Label incorporation into the glycogen C1 was apparent soon thereafter (Fig. 1B, middle trace) followed by label incorporation into a resonance that was clearly resolved from the glycerol C1, C3 resonance. This resonance was assigned to the glycogen C6 (Fig. 1B, top trace) based on its chemical shift of 61.4 p.p.m. [28] and that the linewidth was $\approx$77 Hz (after 20 Hz linebroadening), which was clearly broader than the glucose resonances. The nearby glucose resonances were not

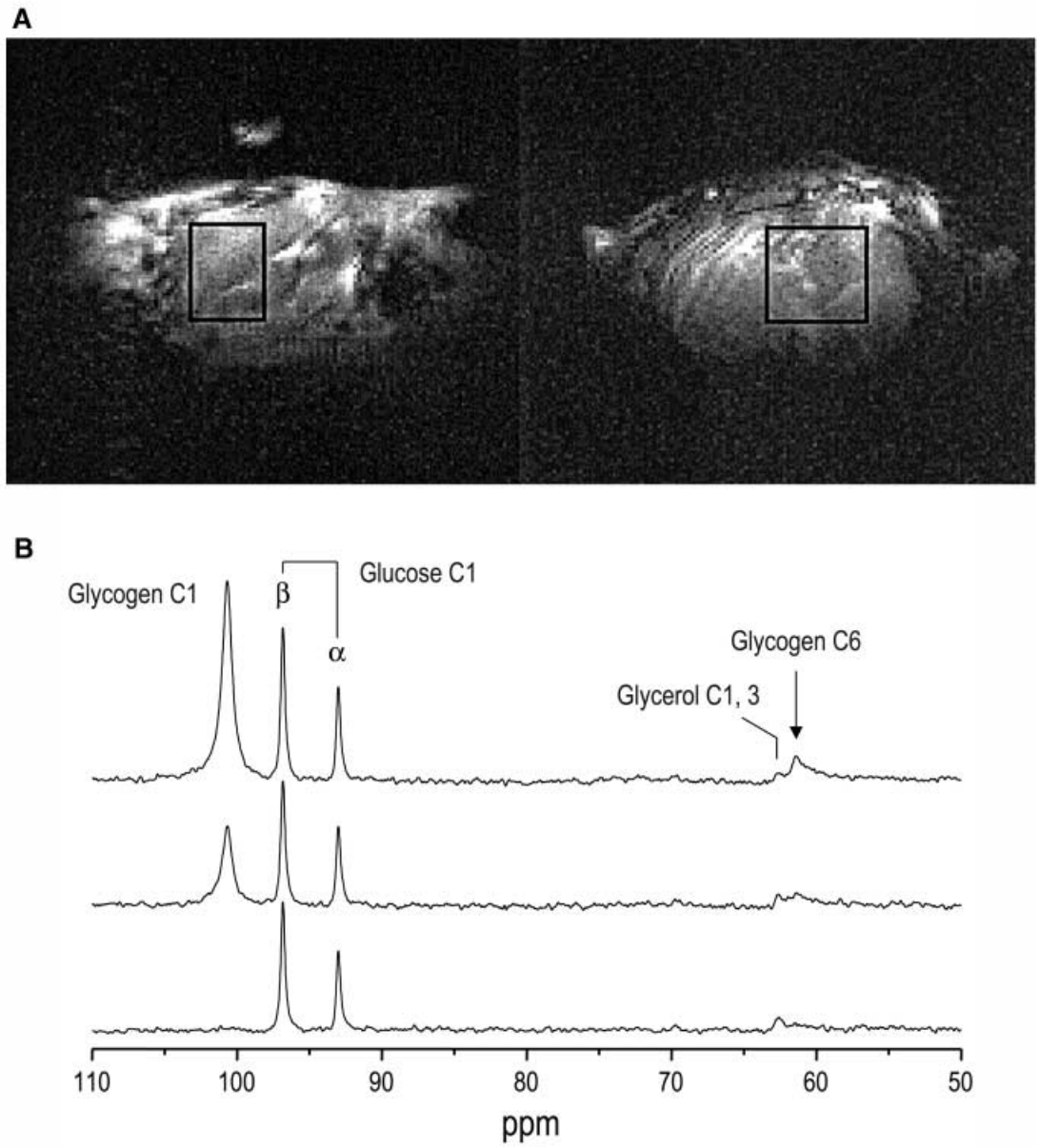


**Fig. 1. $^{1}$H MRI and $^{13}$C MRS of the mouse liver.** (A) Sagittal (left) and transverse (right) images of the liver of a control mouse acquired using the FLASH sequence (TR = 10 ms, TE = 5 ms). The rectangles indicate the location of the volume of interest, ≈400 μL (8.5 × 8 × 6 mm$^3$). The $^{13}$C-labeled formic acid sphere can be seen on the left. (B) Three-dimensional localized $^{13}$C NMR spectra were acquired from a nominal 400 μL volume of the control mouse liver during infusion of [1-$^{13}$C]D-glucose. The spectra were acquired 0.1 h (bottom), 1.5 h (middle), and 3 h (top) after the start of the infusion, and each represents an average over 4.3 min (256 scans, 1 s repetition time). Glycogen syntheses via direct and indirect pathways are demonstrated from the increases of signal intensities of glycogen C1 and C6, respectively. Data processing consisted of 15 Hz exponential multiplication, zero filling, FFT and zero-order phase correction. No baseline correction was applied.

expected to contribute to the glycogen C6 signal change, because the continuous infusion of [1-$^{13}$C] glucose will result in a stable isotopic enrichment for plasma (and liver) glucose of only a few percentage at C6, leading to a much weaker signal compared to glycogen C6. The ability to resolve the resonance of glycerol C1, C3 at 62.5 p.p.m. from the resonance of glycogen C6 allowed, for the first time, the measurement of glycogen C6 changes *in vivo*, which reflects the indirect pathway.

$^{13}$C NMR spectra were acquired while infusing [1-$^{13}$C] glucose in an ADM mouse over 7.6 h (Fig. 2). The glucose level in the liver was maintained at 9.7 ± 0.6 μmol·g$^{-1}$ (mean ± SE, $n$ = 6, control mice) and at 9.1 ± 0.5 μmol·g$^{-1}$ (mean ± SE, $n$ = 6, ADM mice) throughout the experiments. The $^{13}$C-label incorporation into hepatic glycogen C1 and C6 increased at a nearly constant rate for the entire measurement period (Fig. 2).

In addition to the signal increases in glycogen C1 and C6, increased signals were observed in the spectral region from 70 to 78 p.p.m. containing the glycogen C2 through C5 resonances (Fig. 2A), which is enlarged in Fig. 2B. The increase of these signals is consistent with the spectral

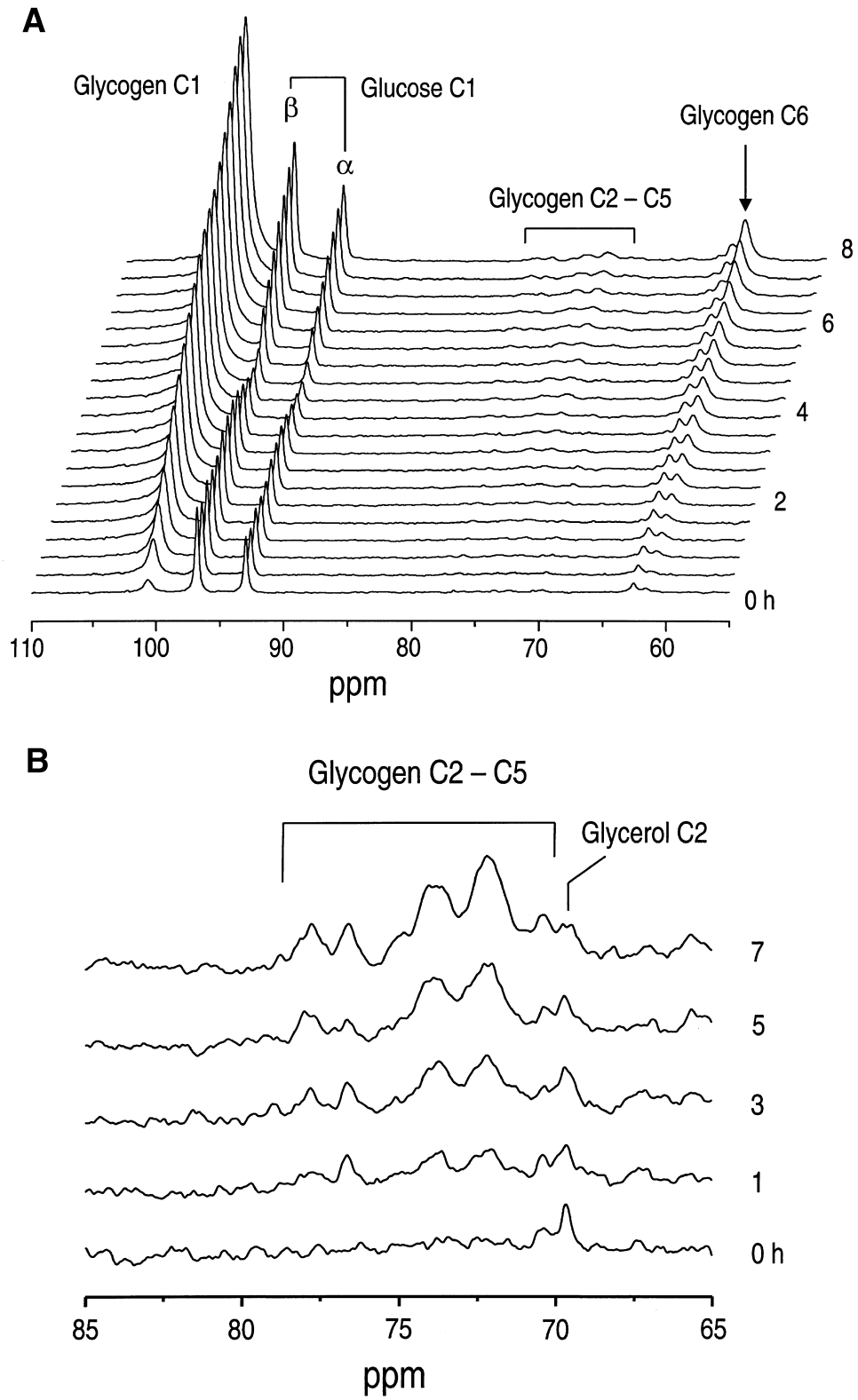


**Fig. 2. Hepatic glycogen synthesis with [1-$^{13}$C]glucose infusion in an ADM mouse.** (A) The stack plot of $^{13}$C spectra acquired over 7.6 h after beginning at $t = 0$ (right scale), the infusion of [1-$^{13}$C]glucose. $^{13}$C-label incorporation into hepatic glycogen was detected in the glycogen C1 and C6 resonances. Net synthesis of glycogen in the liver is visible from the natural abundance signal increase of glycogen C2–C5. The resonance of glycerol C1 and C3 at 62.5 p.p.m. was resolved downfield from the signal of glycogen C6 at 61.4 p.p.m. (B) The region containing the glycogen C2–C5 signals (from Fig. 2A) was expanded vertically to demonstrate the net synthesis of hepatic glycogen during infusion of glucose. Each spectrum corresponds to a 17-min acquisition period. Processing consisted of 20 Hz exponential multiplication, with zero filling, FFT and zero-order phase correction. The spectra are shown without any baseline correction.

pattern of natural abundance glycogen in this region (not shown) and thus was assigned to reflect primarily increases in total hepatic glycogen. This analysis was based on the integration of all the C2–C5 glycogen signals. To determine the potential labeling of the glycogen C2 and C5 resonance due to label scrambling from pyruvate carboxylase/phospho*enol*pyruvate carboxykinase activity ('pyruvate recycling'), the intensity of glycogen C4 was compared to the sum of the C2, C3, C4 and C5 resonances. This comparison showed that glycogen C4 had the same time course (data not shown), indicating that pyruvate recycling had a negligible contribution to the labeling of glycogen under the conditions of our experiment. Natural abundance signals of glycogen were acquired for 30 min before the [1-$^{13}$C] glucose infusion was begun and the quantification yielded a total glycogen of 246 ± 45.5 μmol·g$^{-1}$ (mean ± SE, $n = 6$) in control and 118 ± 27.3 μmol·g$^{-1}$ (mean ± SE, $n = 6$) in ADM mice.

Time-resolved *in vivo* measurements of $^{13}$C-labeled glycogen and glucose in the normal (Fig. 3A) and the ADM (Fig. 3B) mouse liver during 4 h of infusion showed that label incorporation into glycogen C6 lagged compared to

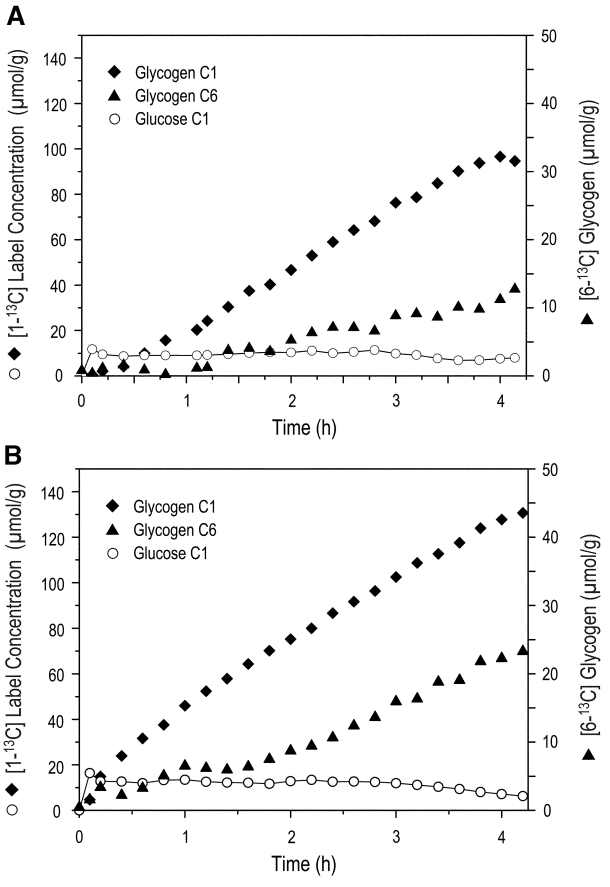


**Fig. 3. Time course of label incorporation into hepatic glycogen and glucose in control and ADM mice.** (A) Representative time courses of glycogen and glucose from the control mouse liver. (B) Representative time courses of glycogen and glucose from the ADM mouse liver. The concentrations of glycogen C1 and glucose C1 resonances are scaled on the left axis and the concentration of glycogen C6 resonance is scaled on the right axis. The spectra used for this plot were averaged to a temporal resolution of 8.5 min (512 scans, 1 s repetition time).

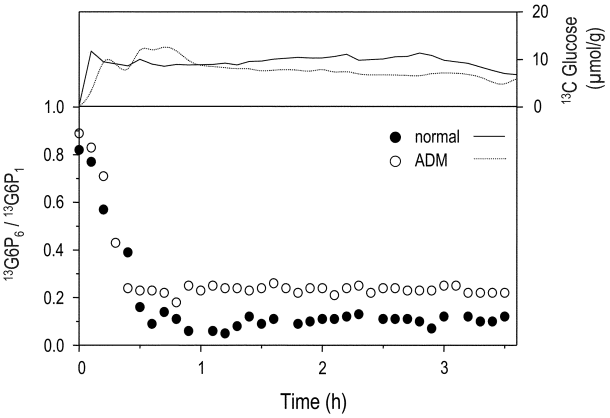


**Fig. 4. Isotopic steady-state at the Glc6*P* level in the liver *in vivo*.** $^{13}$Glc6$P_6$/$^{13}$Glc6$P_1$ is approximated by the ratio of the glycogen C6 to the C1 concentration, $^{13}$Glyc$_6$/$^{13}$Glyc$_1$ (Eqn 7); shown is a control mouse (closed circles) and an ADM mouse (open circles) plotted together with the [1-$^{13}$C]hepatic glucose concentration (top box, with scale to the right) for the control (solid line) and ADM mouse (dashed line). $^{13}$C glucose concentration in the liver was maintained at about 10 μmol·g$^{-1}$ in both groups as shown in the top plot.

that into glycogen C1 in both groups, consistent with the requirement to reach isotopic equilibrium in the glycolytic intermediates downstream of Glc6*P* such as at the level of the trioses. The ratio of change in glycogen C6 relative to that in glycogen C1 reflects the relative isotopic enrichment of Glc6*P* at C6 relative to C1 (Eqn 7). At natural abundance, the ratio is one and decreases to a steady-state value after an initial equilibration period. This results in a transient change in the Glyc$_6$/Glyc$_1$ ratio, even when the equilibration of the Glc6*P* pool was instantaneous. Therefore, the time required to achieve isotopic steady-state at the Glc6*P* level was faster than the 0.61 ± 0.05 h required for Glyc$_6$/Glyc$_1$ to approach steady-state (Fig. 4). From the ratio of glycogen C6 and C1 (Glyc$_6$/Glyc$_1$), we conclude that the relative isotopic enrichment in C6 of Glc6*P* was significantly higher in ADM than that in control mice.

The rate of $^{13}$C label incorporation into glycogen C1 (synthase flux) was 22 ± 1.5 μmol·g$^{-1}$·h$^{-1}$ (mean ± SE) in the control group and 24 ± 1.8 μmol·g$^{-1}$·h$^{-1}$ in the ADM group, which was not statistically different between the two groups ($n = 6$, p = 0.34, two-tailed *t*-test, Fig. 5). However, the rate of label incorporation into glycogen C6 was significantly lower in the control (3.7 ± 0.5 μmol·g$^{-1}$·h$^{-1}$, mean ± SE) compared to the ADM group (5.6 ± 0.5 μmol·g$^{-1}$·h$^{-1}$, mean ± SE) ($n = 6$, p = 0.02). The rate of net glycogen synthesis was significantly lower in the control group (47.2 ± 6.5 μmol·g$^{-1}$·h$^{-1}$) than the ADM group (95.7 ± 19.9 μmol·g$^{-1}$·h$^{-1}$) ($n = 6$, p = 0.04). Overall the rates of glycogen metabolism in the control group were lower than those in the ADM group.

## DISCUSSION

In this study, changes in hepatic carbohydrate metabolism due to the alteration of the activity of bifunctional enzyme 6-phosphofructo-2-kinase/fructose-2,6-bisphosphatase were monitored using 3D-localized $^{13}$C NMR spectroscopy.

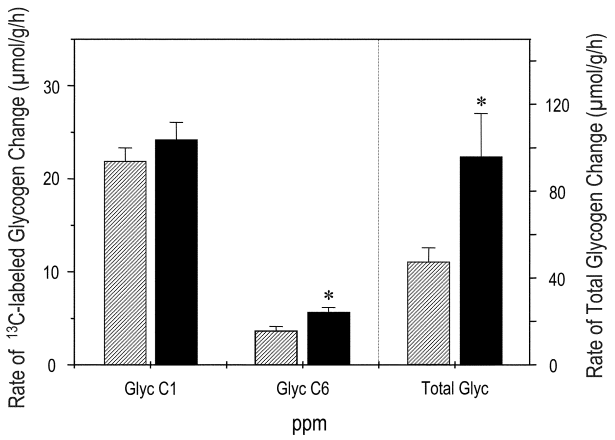


**Fig. 5. Rate of glycogen C1, C6 and net glycogen changes during [1-$^{13}$C]glucose infusion in the mouse liver *in vivo*.** The rates of glycogen C1 and C6 changes were plotted in the left two pairs of bar graphs (left axis) and the rate of net glycogen changes was plotted in the right pair of bar graphs (right axis). The hatched columns are from the control group ($n = 6$) and the solid columns are from the ADM group ($n = 6$). The rate changes were calculated by linear regression. Data are shown in mean ± SE (error bars). * denotes statistically significant difference in means based on a two-tailed *t*-test ($P < 0.05$, $n = 6$).

Because of its high concentration in hepatic tissue leading to a high sensitivity, the study focused on the measurement of the glycogen signals. This study represents several novel advances in *in vivo* NMR methodology. First, the challenges presented by measuring a well-defined volume of hepatic tissue in the small liver volume were overcome using a three-dimensional localization method in conjunction with an RF coil design optimized for the mouse liver and very high magnetic field, 9.4 Tesla. Although challenges remain in shimming the signals from the mouse liver, localization was important to eliminate potential signal sources from non-hepatic tissue, which was accomplished by a well-defined volume of interest that concomitantly improved spectral quality. This was evident from the separation of the glycogen C6 and glycerol C1, C3 signals, an achievement that, to our knowledge, has not been achieved in the intact liver *in vivo*. The importance of the detection of label incorporation into glycogen C6 while infusing [1-$^{13}$C]glucose can be appreciated from the fact that this labeling pattern is only possible due to activity of the indirect pathway of glycogen synthesis. In addition, this study reports for the first time the simultaneous detection of increased signal intensity for the glycogen C2–C5 resonances. These changes in intensity were attributed to increases in the natural abundance glycogen concentration, based on the observation that the rate of the glycogen C4 signal intensity changed in parallel with the signal intensity of all C2–C5 resonances, and that the spectra shown in Fig. 2B closely resembled those of natural abundance glycogen in aqueous solutions. Therefore, this study reports the first simultaneous measurements of label incorporation into glycogen C1 and C6, as well as changes in total glycogen content *in vivo*, which can be used to assess the activity of the direct and indirect pathway, as well as net glycogen changes.

To our knowledge, this is also the first study to apply this technology to adenovirus transfected mouse liver. Previously, we reported that the levels of Fru-2,6-$P_2$ were significantly increased by adenovirus-mediated overexpression of a mutant form of 6-phosphofructo-2-kinase/fructose-2,6-bisphosphatase in the mouse liver [8,9]. The increased hepatic Fru-2,6-$P_2$ levels resulted in mild hypoglycemia in normal mice and amelioration of hyperglycemia in diabetic animals. In this study, the impact of hepatic overexpression of 6-phosphofructo-2-kinase/fructose-2,6-bisphosphatase on glucose and glycogen metabolism due to altered hepatic Fru-2,6-$P_2$ levels was monitored using 3D localized $^{13}$C NMR spectroscopy and the results were consistent with our recent *in vitro* measurements [8]. For example, the liver glycogen concentration determined *in vivo* by natural abundance $^{13}$C NMR spectroscopy just prior to infusion of the [1-$^{13}$C] glucose was reduced in the ADM mice relative to the control animals. The lower hepatic glycogen content in the ADM group reflects increased glycogen utilization in an effort of the liver to establish euglycemia and reflects an overexpression of double mutant 6-phosphofructo-2-kinase/fructose-2,6-bisphosphatase in the livers of these mice. Although this is qualitatively consistent with our earlier results [8], the hepatic glycogen content in this study was approximately 20–25% lower than that determined previously *in vitro*, which was attributed to the fact that in contrast to the previous work, in the present study mice were fasted for 8–12 h before the NMR experiments were begun. Together, these results demonstrate that increased Fru-2,6-$P_2$ has similar metabolic effects in the fed as well as in the fasted state. During the NMR experiments, the infusion of [1-$^{13}$C] glucose was sufficient to maintain blood glucose levels between 10 and 12 mM to induce hyperglycemic states similar to diabetes. The glycogen repletion observed in both the control and ADM groups was consistent with transition from the fasted to the hyperglycemic (fed) states. The striking linearity of the signal increase of glycogen C1 and C6 during this long measurement period (Fig. 3) implies measurement of either the early phase of turnover, as the curve did not show any evidence for a leveling of the signal (which suggests a surprisingly long turnover time), or net synthesis of glycogen or the combination of both.

The rates of total glycogen synthesis and $^{13}$C label incorporation into glycogen (Fig. 5) suggest that the overall rate of glycogen synthesis is much higher than the rate at which the labeled glucose is incorporated into the newly synthesized glycogen. This result was unexpected, since the amount of label transferred into glycogen should reflect turnover as well as synthesis and thus be higher than the rate of net glycogen synthesis. This observation can be explained, however, by assuming that the isotopic enrichment of Glc6*P* was much lower than that of glucose. A lower enrichment of Glc6*P* relative to glucose may be due to a slow rate of glucose phosphorylation, or dilution by extra-hepatic precursors and an active indirect pathway of glycogen synthesis. Previous work suggests that the latter situation is more likely, as increased hepatic Fru-2,6-$P_2$ was associated with an up-regulation of glucokinase and a down-regulation of Glc6*P*ase gene expression [8]. These observations are also consistent with previous reports suggesting that 30% to 70% of the postprandial liver glycogen is from the indirect pathway [29–31].

Although the increased hepatic Fru-2,6-$P_2$ produced by the ADM treatment promoted a higher rate of net glycogen

synthesis when compared to the normal control mice, the rate of [1-$^{13}$C] glucose incorporation was not significantly increased. However, the rate of $^{13}$C incorporation into the C6 position in glycogen was significantly increased in the ADM group, which suggests that the indirect pathway for glycogen deposition was activated in response to increased hepatic Fru-2,6-$P_2$. This is a surprising result when considering that the putative effect of Fru-2,6-$P_2$ is to activate 6-phosphofructo-1-kinase and inhibit fructose-1,6-bisphosphatase, which should have reduced the activity of the indirect pathway of glycogen synthesis, as it depends on flux through fructose-1,6-bisphosphatase. However, it is likely that the increased rate of $^{13}$C label incorporation into the C6 position of glycogen in the ADM group is indicative of activated 6-phosphofructo-1-kinase, which can lead to increased $^{13}$C labeling at the triose level. Such a mechanism can lead to increases in labeling of glycogen C6 even in the presence of decreased activity of the indirect pathway, provided that the increase in glycolytic flux exceeded the decreased gluconeogenic flux substantially. The ability of the liver to replenish glycogen stores via the indirect pathway, even in the face of high Fru-2,6-$P_2$ levels, suggests that the activation of 6-phosphofructo-1-kinase by this biofactor is more potent than its inhibition of fructose-1,6-bisphosphatase. This is a significant observation because it offers the first *in vivo* assessment of the action of Fru-2,6-$P_2$ on the 6-phosphofructo-1-kinase/fructose-1,6-bisphosphatase cycle. The result must be interpreted with care, however, as both glycolysis and glycogen synthesis have been shown to be influenced by substrate channeling and protein–protein interactions [32–34]. Such mechanisms may provide for effective 'pooling' of glycolytic/glycogenic precursors, i.e. Glc6*P*.

In summary, based on several substantial advances in the $^{13}$C NMR methodology, the observation of simultaneously enhanced indirect hepatic glycogen synthesis and glycolysis in the ADM group has clarified the *in vivo* action of Fru-2,6-$P_2$ on the 6-phosphofructo-1-kinase/fructose-1,6-bisphosphatase cycle, suggesting that the activation of glycolysis predominates over the inhibition of gluconeogensis. These data, in conjunction with our earlier reports, strongly suggest that the bifunctional enzyme is an enticing target for antidiabetic therapies aimed at increasing hepatic Fru-2,6-$P_2$ content.

## ACKNOWLEDGEMENTS

This study was supported by the NIH grants R01DK38354 (A. J. L.) and two Grants-in-Aid by the University of Minnesota Graduate School (R. G., A. J. L.). Purchase of 9.4 Tesla magnet was partially supported by a gift from the W. M. Keck Foundation and the Center for MR research is in part supported by a biotechnology research program grant from the National Center for Research Resources, P41RR08079.

## REFERENCES

1. Nordlie, R.C., Foster, J.D. & Lange, A.J. (1999) Regulation of glucose production by the liver. *Annu. Rev. Nutr.* **19**, 379–406.
2. Cherrington, A.D. (1999) Banting Lecture 1997. Control of glucose uptake and release by the liver *in vivo*. *Diabetes* **48**, 1198–1214.
3. Okar, D.A., Lange, A.J., Manzano, A., Navarro-Sabate, A., Riera, L. & Bartrons, R. (2001) PFK-2/FBPase-2: maker and breaker of the essential biofactor fructose-2,6-bisphosphate. *Trends. Biochem. Sci.* **26**, 30–35.
4. Pilkis, S.J., Chrisman, T., Burgress, B., McGrane, M., Colosia, A., Pilkis, J., Claus, T.H. & el-Maghrabi, M.R. (1983) Rat hepatic 6-phosphofructo 2-kinase/fructose 2,6-bisphosphatase: a unique bifunctional enzyme. *Adv. Enzyme. Regul.* **21**, 147–173.
5. Van Schaftingen, E. & Hers, H.G. (1981) Phosphofructokinase 2: the enzyme that forms fructose 2,6-bisphosphate from fructose 6-phosphate and ATP. *Biochem. Biophys. Res. Commun.* **101**, 1078–1084.
6. Pilkis, S.J., el-Maghrabi, M.R. & Claus, T.H. (1988) Hormonal regulation of hepatic gluconeogenesis and glycolysis. *Annu. Rev. Biochem.* **57**, 755–783.
7. El-Maghrabi, M.R., Pate, T.M., Murray, K.J. & Pilkis, S.J. (1984) Differential effects of proteolysis and protein modification on the activities of 6-phosphofructo-2-kinase/fructose-2,6-bisphosphatase. *J. Biol. Chem.* **259**, 13096–13103.
8. Wu, C., Okar, D.A., Newgard, C.B. & Lange, A.J. (2001) Overexpression of 6-phosphofructo-2-kinase/fructose-2,6-bisphosphatase in mouse liver lowers blood glucose by suppression of hepatic glucose production. *J. Clin. Invest.* **107**, 91–98.
9. Wu, C., Okar, D.A., Newgard, C.B. & Lange, A.J. (2002) Increasing fructose 2,6-bisphosphate overcomes hepatic insulin resistance of type 2 diabetes. *Am. J. Physiol. Endocrinol. Metab.* **282**, E38–E45.
10. Kurland, I.J., el-Maghrabi, M.R., Correia, J.J. & Pilkis, S.J. (1992) Rat liver 6-phosphofructo-2-kinase/fructose-2,6-bisphosphatase. Properties of phospho- and dephospho- forms and of two mutants in which Ser32 has been changed by site-directed mutagenesis. *J. Biol. Chem.* **267**, 4416–4423.
11. Tauler, A., Lin, K. & Pilkis, S.J. (1990) Hepatic 6-phosphofructo-2-kinase/fructose-2,6-bisphosphatase. Use of site-directed mutagenesis to evaluate the roles of His-258 and His-392 in catalysis. *J. Biol. Chem.* **265**, 15617–15622.
12. Cohen, S.M., Ogawa, S. & Shulman, R.G. (1979) 13C NMR studies of gluconeogenesis in rat liver cells: utilization of labeled glycerol by cells from euthyroid and hyperthyroid rats. *Proc. Natl Acad. Sci. USA* **76**, 1603–1609.
13. Cohen, S.M., Rognstad, R., Shulman, R.G. & Katz, J. (1981) A comparison of $^{13}$C nuclear magnetic resonance and 14C tracer studies of hepatic metabolism. *J. Biol. Chem.* **256**, 3428–3432.
14. Cohen, S.M. (1983) Simultaneous $^{13}$C and $^{31}$P NMR studies of perfused rat liver. Effects of insulin and glucagon and a $^{13}$C NMR assay of free $Mg^{2+}$. *J. Biol. Chem.* **258**, 14294–14308.
15. Iles, R.A., Griffiths, J.R., Stevens, A.N., Gadian, D.G. & Porteous, R. (1980) Effects of fructose on the energy metabolism and acid-base status of the perfused starved-rat liver. A 31phosphorus nuclear magnetic resonance study. *Biochem. J.* **192**, 191–202.
16. Shulman, G.I., Rothman, D.L., Smith, D., Johnson, C.M., Blair, J.B., Shulman, R.G. & DeFronzo, R.A. (1985) Mechanism of liver glycogen repletion *in vivo* by nuclear magnetic resonance spectroscopy. *J. Clin. Invest.* **76**, 1229–1236.
17. Shulman, G.I., Rossetti, L., Rothman, D.L., Blair, J.B. & Smith, D. (1987) Quantitative analysis of glycogen repletion by nuclear magnetic resonance spectroscopy in the conscious rat. *J. Clin. Invest.* **80**, 387–393.
18. Rothman, D.L., Magnusson, I., Katz, L.D., Shulman, R.G. & Shulman, G.I. (1991) Quantitation of hepatic glycogenolysis and gluconeogenesis in fasting humans with $^{13}$C NMR. *Science* **254**, 573–576.
19. Magnusson, I., Rothman, D.L., Jucker, B., Cline, G.W., Shulman, R.G. & Shulman, G.I. (1994) Liver glycogen turnover in fed and fasted humans. *Am. J. Physiol.* **266**, E796–E803.
20. Roden, M., Perseghin, G., Petersen, K.F., Hwang, J.H., Cline, G.W., Gerow, K., Rothman, D.L. & Shulman, G.I. (1996) The

roles of insulin and glucagon in the regulation of hepatic glycogen synthesis and turnover in humans. *J. Clin. Invest*. **97**, 642–648.
21. Petersen, K.F., Laurent, D., Rothman, D.L., Cline, G.W. & Shulman, G.I. (1998) Mechanism by which glucose and insulin inhibit net hepatic glycogenolysis in humans. *J. Clin. Invest*. **101**, 1203–1209.
22. David, M., Petit, W.A., Laughlin, M.R., Shulman, R.G., King, J.E. & Barrett, E.J. (1990) Simultaneous synthesis and degradation of rat liver glycogen. An *in vivo* nuclear magnetic resonance spectroscopic study. *J. Clin. Invest*. **86**, 612–617.
23. Adriany, G. & Gruetter, R. (1997) A half Volume coil for efficient proton decoupling in humans at 4 Tesla. *J. Magn. Reson*. **125**, 178–184.
24. Choi, I.-Y., Tkac, I. & Gruetter, R. (2000) Single-shot, three-dimensional 'non-echo' localization method for *in vivo* NMR spectroscopy. *Magn. Reson. Med*. **44**, 387–394.
25. Gruetter, R., Ugurbil, K. & Seaquist, E.R. (1998) Steady-state cerebral glucose concentrations and transport in the human brain. *J. Neurochem*. **70**, 397–408.
26. Choi, I.-Y., Tkac, I., Ugurbil, K. & Gruetter, R. (1999) Non-invasive measurements of [1-$^{13}$C] glycogen concentrations and metabolism in rat brain *in vivo*. *J. Neurochem*. **73**, 1300–1308.
27. Watanabe, H. & Passonneau, J.V. (1973) Factors affecting the turnover of cerebral glycogen and limit dextrin *in vivo*. *J. Neurochem*. **20**, 1543–1554.
28. Canioni, P. & Quistorff, B. (1994) *Liver Physiology and Metabolism in NMR in Physiology and Biomedicine*, pp. 373–388. Academic Press, San Diego, CA.
29. Magnusson, I. & Shulman, G.I. (1991) Pathways of hepatic glycogen synthesis in humans. *Med. Sci. Sports. Exerc*. **23**, 939–943.
30. Spence, J.T. & Koudelka, A.P. (1985) Pathway of glycogen synthesis from glucose in hepatocytes maintained in primary culture. *J. Biol. Chem*. **260**, 1521–1526.
31. Newgard, C.B., Hirsch, L.J., Foster, D.W. & McGarry, J.D. (1983) Studies on the mechanism by which exogenous glucose is converted into liver glycogen in the rat. A direct or an indirect pathway? *J. Biol. Chem*. **258**, 8046–8052.
32. Yang, R., Cao, L., Gasa, R., Brady, M.J., Sherry, A.D. & Newgard, C.B. (2002) Glycogen-targeting subunits and glucokinase differentially affect pathways of glycogen metabolism and their regulation in hepatocytes. *J. Biol. Chem*. **277**, 1514–1523.
33. O'Doherty, R.M., Jensen, P.B., Anderson, P., Jones, J.G., Berman, H.K., Kearney, D. & Newgard, C.B. (2000) Activation of direct and indirect pathways of glycogen synthesis by hepatic overexpression of protein targeting to glycogen. *J. Clin. Invest*. **105**, 479–488.
34. Agius, L., Centelles, J. & Cascante, M. (2002) Multiple glucose 6-phosphate pools or channelling of flux in diverse pathways? *Biochem. Soc. Trans*. **30**, 38–43.